Carbon 120 (2017) 427–437

Contents lists available at ScienceDirect

Carbon

journal homepage: www.elsevier.com/locate/carbon

A theoretical study on the piezoresistive response of carbon nanotubes embedded in polymer nanocomposites in an elastic region

Hamid Souri [a], Jaesang Yu [b], Haemin Jeon [c], Jae Woo Kim [b], Cheol-Min Yang [b], Nam-Ho You [a, **], B.J. Yang [b, *]

[a] Carbon Composite Materials Research Center, Institute of Advanced Composite Materials, Korea Institute of Science and Technology (KIST), 92 Chudong-ro, Bongdong-eup, Wanju-gun, Jeonbuk, 55324, Republic of Korea
[b] Multifunctional Structural Composite Research Center, Institute of Advanced Composite Materials, Korea Institute of Science and Technology (KIST), 92 Chudong-ro, Bongdong-eup, Wanju-gun, Jeonbuk, 55324, Republic of Korea
[c] Department of Civil and Environmental Engineering, Hanbat National University, 125 Dongseodae-ro, Yuseong-gu, Daejeon, 305-719, Republic of Korea

ARTICLE INFO

Article history:
Received 9 February 2017
Received in revised form
10 May 2017
Accepted 16 May 2017
Available online 17 May 2017

Keywords:
Piezoresistive
Multi-walled carbon nanotubes
Effective medium theory
Electrical conductivity
Polymeric nanocomposite

ABSTRACT

Herein, we report a theoretical study of polymeric nanocomposites to provide physical insight into complex material systems in elastic regions. A self-consistent scheme is adopted to predict piezoresistive characteristics, and the effects of the interface and of tunneling on the effective piezoresistive and electrical properties of the nanocomposites are simulated. The overall piezoresistive sensitivity is predicted to be reduced when the lower interfacial resistivity of multi-walled carbon nanotubes (MWCNTs) and the higher effective stiffness of nanocomposites are considered. In addition, thin film nanocomposites with various MWCNT weight percentages are manufactured and their electrical performance capabilities are measured to verify the predictive capability of the present simulation. From experimental tests, the nanocomposites show clear piezoresistive behaviors, exhibiting a percolation threshold at less than 0.5 wt% of the MWCNTs. Three sets of comparisons between the experimental data and the present predictions are conducted within an elastic range, and the resulting good correlations between them demonstrate the predictive capability of the present model.

1. Introduction

Over the past decade, functional composites consisting of nano-scale materials and polymers have attracted extensive attention due to their significant impact on industrial applications [1]. In particular, the carbon nanotube (CNT) filler in the polymer matrix can enhance both the mechanical and electrical characteristics, resulting in composites with better properties compared to those of the pure polymer [2]. The enhanced characteristics can provide functional properties of CNT-reinforced nanocomposites (*e.g.*, piezoresistive response), and they are mostly originated from the CNT filler [3,4]. However, the changes and complexity in the polymer characteristics with the addition of CNTs are poorly understood, which restricts precise predictions of the multi-physical behavior of nanocomposites [5]. Hence, understanding the nature of multi-physical responses from functional nanomaterials is critical to design and utilize the nanomaterial in actual applications [6–8].

To date, various attempts have been made to model the physico-chemical effects of nanoscale fillers on the electro-mechanical and/or piezoresistive behaviors of nanocomposite materials. However, most of the studies in the theoretical fields have focused on separate predictions for each phenomenon. Wang et al. [9] proposed a continuum model based on an effective medium theory that describes the electrical conduction process in CNT-reinforced nanocomposites [9]. Furthermore, the model was recently extended by Ref. [10] in order to simulate the electrical properties of graphene nanocomposites [10]. Although the above-mentioned studies demonstrated that the newly developed models successfully captured the quantitative behavior of nanocomposites, such as elastic modulus, electrical conductivity, and percolation threshold, the consideration of the relation between electrical-mechanical behaviors was not included. Generally, two kinds of methods are often utilized to simulate the piezoresistive responses of polymer-

* Corresponding author.
** Corresponding author.
E-mail addresses: polymer@kist.re.kr (N.-H. You), bj.yang@kist.re.kr (B.J. Yang).

http://dx.doi.org/10.1016/j.carbon.2017.05.059
0008-6223/

based composites. The first one can be referred to as numerical network model that is based on a combined three-dimensional statistical method and fiber reorientation technique [11,12]. The numerical network model has an advantage that can consider piezoresistive response under both tensile and compressive loading; however, the numerical network model does not reflect the hardness of materials, which limits the application of the current composite system. The second method is the analytical microscale formulation [13,14], which can be implemented into the finite element (FE) -based system to analyze engineering problems [15,16]. Nevertheless, these approaches also remain limited due to their inherent characteristic that may describe a simple uniaxial tensile loading and difficult to predict the inherent nanoscopic characteristics.

In addition, researchers have developed various piezoresistive materials based on polymeric matrices with the incorporation of conductive fillers, such as carbon fibers [17], carbon black [18], graphite [19], and CNTs [20–24]. Among all these conductive fillers, CNTs have attracted the most attention to be used in piezoresistive composites due to their dramatic change of electrical conductivity under external load [25] and thus, polymer nanocomposites containing CNTs have been widely employed for their great piezoresistive, mechanical, and electrical properties [25,26].

For instance, the incorporation of 8 wt% of multi-walled carbon nanotubes (MWCNTs) and single-walled carbon nanotubes (SWCNTs) in the polyurethane matrix resulted in 5–50% of electrical resistance change under 35–40% of applied tensile strain, respectively [27]. In another study, the piezoresistive characteristics of MWCNTs within thermoplastic polyurethane (TPU) were studied under cyclic compression strains up to 90% [28]. In another research work [29], showed that 0.05 wt% of SWCNTs in polyimide (PI) matrix resulted in 2% electrical resistance change under 16 MPa of applied tensile stress, while the electrical resistance of a 10 wt% MWCNT/PI system altered up to 0.35% under similar loading conditions [29]. Moreover [30], studied the piezoresistive characteristics of epoxy-based nanocomposites using MWCNTs as conductive nano-fillers under applied tensile load. In accordance with their results, as the MWCNT loading was increased from 0.1 to 0.5 wt%, the electrical resistance change rate increased from 7 to 12% [30]. In another work, the piezoresistive response of MWCNTs/polysulfone (PSF) nanocomposite film was obtained. The 0.5 wt% of MWCNTs filled in PSF showed the electrical resistance change of 18% under applied tensile fracture strain of 3.5% [21].

However, most of the polymers used for the fabrication of piezoresistive composites were mechanically and thermally weak to be used in applications in harsh environments with high temperatures. Aromatic PIs are high-performance polymers with a number of outstanding properties, such as a low dielectric constant, high thermal stability, and favorable chemical and mechanical properties [31,32]. In previous studies, it was shown that the addition of CNTs could effectively enhance the thermal properties of the CNT/PI nanocomposites [33,34]. For instance, in Ref. [31], the TGA results support the fact that the CNT/PI nanocomposites are highly thermally stable. This suggests the idea that the CNT/PI piezoresistive sensors can be used in harsh environments with high temperatures.

In the present study, the piezoresistive response predictions were carried out based on the self-consistent effective medium theory that accounts for the interface and tunneling effects. With the derived formulation, the effects of the MWCNT weight percentages, lengths, and tunneling effects on the piezoresistivity of the nanocomposites were discussed in detail. The novelty of the present model is in the flexibility and simplicity of the derivation to represent the piezoresistive response with a limited number of model parameters. In addition, it is straightforward to extend the proposed model for use as a user-defined material (UMAT) with implementation into the finite element method (FEM) to predict a more complex structural system. The capability of the present model to predict the overall electrical behaviors of nanocomposites is demonstrated through a number of parametric investigations. Furthermore, MWCNT/PI films with various weight percentages of MWCNTs were fabricated for validation purposes. A doctor-blade method was used to fabricate piezoresistive specimens, and their electrical and mechanical properties were correspondingly evaluated by a four-point probe method and by uniaxial tensile testing. Comparisons between the experimental data and the predictions based on the present theoretical study were then carried out for a further demonstration of the capability of the proposed model.

2. Theory

2.1. Piezoresistive response of nanocomposites considering interface and tunneling effects

A self-consistent effective medium theory is introduced here to predict the effective piezoresistive behavior of nanocomposites. The effective medium theory [9,10] is adopted to model electrical conductivity of nanocomposites containing MWCNTs with imperfect interfaces, and the tunneling model is modified in this study to represent piezoresistivity characteristics. Key features of the present study and comparisons with senior author's papers are addressed below.

The piezoresistive response of nanocomposites has been modeled by a filler orientation-based method in previous papers [5,10–13]. However, the methods published literature may not be suitable for the stiffer polymer- and/or ceramic-based composites (*e.g.*, polyimide and cement) since the displacement levels of those materials are very small (less than 2–3 mm). Despite the low level of filler and external deformation, piezoresistivity can be confirmed by various experimental results [28,35], and the insoluble phenomena is attributed by the tunneling effect [22]. In this study, therefore, the sensitivity of piezoresistivity of nanocomposites is assumed to be simulated by choosing an appropriate scale parameter of tunneling, denoted by γ.

First, let us consider the two-phase composite composed of the matrix (phase 0) with the electrical conductivity σ_0, and 3D randomly oriented ellipsoidal CNTs (phase 1) with the electrical conductivity σ_1. In order to understand and predict the piezoresistive behavior on the MWCNT/PI films, we conducted the effective medium theory-based simulation. In the present study, the fillers are assumed to be non-interacting and embedded firmly in the matrix [36,37]. Then, the medium representative volume element (RVE) of two-phase composites containing arbitrary non-aligned fillers can be represented by Refs. [9,10,59].

$$\phi_0\left[\left(\sigma_0-\sigma^*\right)^{-1}+\mathbf{S}_0\left(\sigma^*\right)^{-1}\right]^{-1}+\phi_1\left[\left(\sigma_1-\sigma^*\right)^{-1}+\mathbf{S}_1\left(\sigma^*\right)^{-1}\right]^{-1}=0 \tag{1}$$

where ϕ_r denotes the volume fraction of the r-phase ($r=0,1$) and σ^* is the effective electrical conductivity (electrical conductivity of composites). $\mathbf{S}$ is the shape-dependent depolarization tensors of associated phases [10]. Since the matrix shape is envisioned to be spherically symmetric, the components of $\mathbf{S}_0$ are defined as 1/3 in all direction [9]; while $\mathbf{S}_1$ for ellipsoidal CNT fillers with a symmetric axis 3 are explicitly given as [38]

$$S_{11} = S_{22} = \begin{cases} \dfrac{\alpha}{2\left(1-\alpha^2\right)^{1.5}}\left[\cos^{-1}\alpha - \alpha\left(1-\alpha^2\right)^{0.5}\right], \alpha < 1 \\ \dfrac{\alpha}{2\left(\alpha^2-1\right)^{1.5}}\left[\alpha\left(\alpha^2-1\right)^{0.5} - \cosh^{-1}\alpha\right], \alpha > 1 \end{cases} \tag{2}$$

where α signifies the aspect ratio (length-to-diameter) and $S_{33} = 1-2S_{11}$ [38].

Substituting Eq. (2) into Eq. (1) yields the implicit equation of the effective electrical conductivity (σ^*) for CNTs-reinforced nanocomposites with interface effects as [10]

$$\frac{3(1-\phi_1)(\sigma_0-\sigma^*)}{\sigma_0+2\sigma^*} + \frac{\phi_1}{3}\left\{\frac{2(\sigma_{11}^c-\sigma^*)}{\sigma^*+(\sigma_{11}^c-\sigma^*)+S_{11}} + \frac{\sigma_{33}^c-\sigma^*}{\sigma^*+(\sigma_{33}^c-\sigma^*)+S_{33}}\right\} = 0 \tag{3}$$

By following the method proposed by Ref. [9], all fillers are assumed to be thinly coated with interface region, σ_{ii}^c, and it can be expressed as [9,10]:

$$\sigma_{ii}^c = \frac{r\alpha\sigma_{ii}}{r\alpha + S_{ii}\sigma_{ii}(1+2\alpha)\rho(\phi_1)} \tag{4}$$

where σ_{ii} and r are the electrical conductivity in i-axis ($i = 1, 3$) and radius of CNTs, respectively. It is noted that the straight and randomly oriented MWCNTs are assumed in the current model. In order to achieve more realistic predictions of the proposed model, additional theoretical considerations should be included to explore the morphological effect of MWCNTs on the piezoresistive response of the nanocomposites. The methods are not limited to, but may include theoretical approaches proposed by Refs. [39–41]. Nonetheless, these aspects are not of particular scope in the present work and should be considered in future work.

In addition, to capture the piezoresistive responses, the following assumptions are applied in this simulation: (a) The CNT fillers are interconnected by electron tunneling activity and (b) the field region of the tunneling effect is transformable by the level of material deformation. Based on the abovementioned conditions, the modified Cauchy's probabilistic model is applied here to describe the complicate tunneling phenomenon. Hence, $\rho(\phi_1)$ in Eq. (4) can be written as [10]

$$\rho(\phi_1) = \frac{\rho_0\left[1 - F(\phi_1; \phi_1^*, \gamma(\bar{\varepsilon}))\right]}{\left[1 - F(0; \phi_1^*, \gamma(\bar{\varepsilon}))\right]} \tag{5}$$

with

$$F(\phi_1; \phi_1^*, \gamma(\bar{\varepsilon})) = \frac{1}{\pi}\arctan\left(\frac{\phi_1 - \phi_1^*}{\gamma(\bar{\varepsilon})}\right) + 0.5 \tag{6}$$

and

$$\phi_1^* = \frac{9S_{33}(1-S_{33})}{-9S_{33}^2 + 15S_{33} + 2} \tag{7}$$

where ρ_0 is the parameter of the intrinsic interfacial resistivity between CNTs and the matrix [10]. Following [9,10], the electrical resistance at interfacial region is assumed to be controlled by the value of ρ_0 in the present paper. Since the ρ_0 of MWCNTs-embedded polyimide nanocomposite is not quantified by Refs. [9,10], the constant is estimated by fitting the experimentally obtained resistance change curve with the prediction. Details of the principle of interfacial resistivity can be found in Refs. [9,10,42], and $\gamma(\bar{\varepsilon})$ is the scale parameter correlated with the tunneling effect region that can be expressed as

$$\gamma(\bar{\varepsilon}) = \mathbf{C}^* : \bar{\varepsilon} \tag{8}$$

where $\bar{\varepsilon}$ denotes the averaged strain and $\mathbf{C}^*$ is the effective stiffness tensor of composites. The degree of $\mathbf{C}^*$ can be obtained through both experimental tests and/or theoretical approaches on the basis of micromechanics [60]. In the present study, the experimentally measured elastic modulus under uniaxial tensile stress is utilized to estimate the $\mathbf{C}^*$. It should be noted that the present study is only applicable to elastic regions; thus, $\mathbf{C}^*$can only reflect the elastic mechanical behavior of the composites. In order to predict more complex characteristics such as long-term and/or fatigue properties, it is necessary to consider plastic regions. However, this is beyond the scope of the present study, and additional work will therefore be carried out in the future.

The modified analytical model can be implemented into a finite element (FE) or finite difference (FD) program to simulate boundary problems of various nanocomposites. The numerical efficiency of the simulation can be a key factor for analyzing complex, large-scale composite structures; therefore, a simpler constitutive model is required in the FE or FD implementation. Accordingly, the proposed framework is more suitable for an expandable implementation than previous studies such as [12,14].

2.2. Numerical simulations

A series of numerical simulations are carried out to verify the effectiveness of the proposed model. Specifically, the influences of material and model parameters on the overall piezoresistive behaviors are examined. The same material properties of MWCNTs/PI in the experiment are adopted as: $\sigma_0 = 5E\text{-}15$ S/m, $\sigma_1 = 1.94E4$ S/m, $L = 100$ μm, $D = 4.5$ nm. The interface constant is fixed as $\rho_0 = 6E\text{-}5$ m^2/S and the tensile test results in the experimental section are utilized as the effective stiffness of composite ($\mathbf{C}^*$). It is noted that the electrical conductivity of MWCNTs (σ_1) is provided by the manufacturer data sheet (Wonil Corporation), which is similar to the values in literature [3,43]. In addition, the interfacial resistivity is a model parameter that can be determined by experimental comparison with a trial-and-error procedure.

First, in an attempt to investigate the effect of volume fraction of MWCNTs, the predicted piezoresistive responses under uniaxial tension with various ϕ_1 are shown in Fig. 1(a). The amounts of applied strain on the nanocomposites are depicted in the figure, and it is apparent that the electrical resistance change decreases as the volume faction of MWCNTs increases. The proposed model is further utilized to predict the overall piezoresistive response of nanocomposites with an increase in the length of MWCNTs in Fig. 1(b). It is calculated that the electrical resistance change is more pronounced at the lower length of MWCNTs, and demonstrated in Fig. 1(a) and (b) that the piezoresistive effect of nanocomposites is fairly associated to a certain extent with the volume fraction and length of fillers [44]. This mainly arises due to the reason that the formation of conductivity network pathways is significantly affected by the filler conditions, and can be concluded that relatively well-structured conductivity network leads to less variation of the electrical resistance change of nanocomposites by applied uniaxial tension.

The change in the piezoresistive responses of the

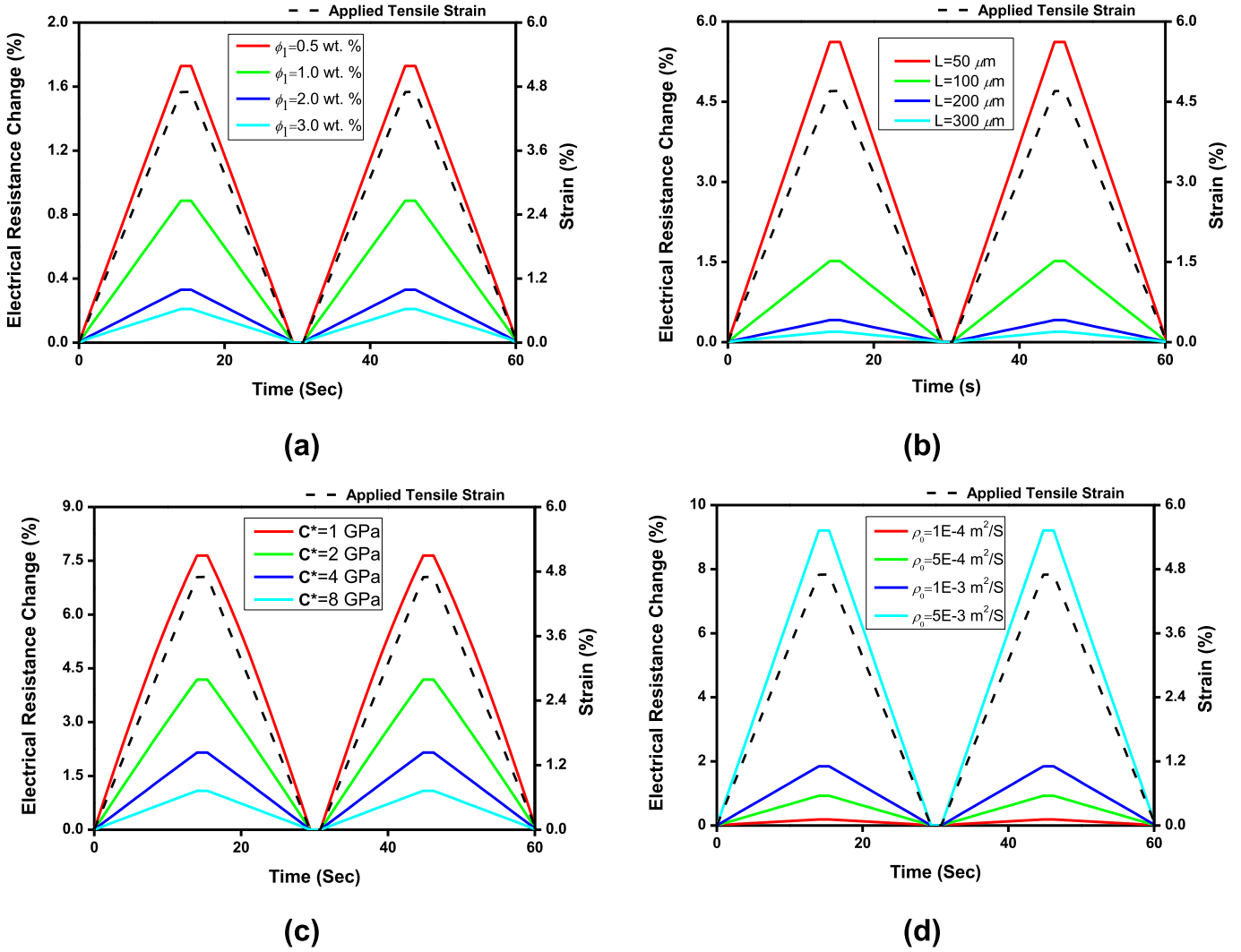

Fig. 1. The numerical simulation results (σ_0 = 5E-15 S/m, σ_1 = 1.943E4 S/m, and D = 4.5 nm): the predicted electrical resistance change with varying (a) weight percentages of MWCNTs, (b) length of MWCNTs, (c) effective stiffness of nanocomposites, and (d) interfacial resistivity between the matrix and MWCNTs. (A colour version of this figure can be viewed online.)

nanocomposite with different strain degrees can be discussed in parallel with the change in the electrical network formation induced by the constitutive materials in composite. When the volume fraction and length of MWCNTs increase, the electrical network is densified by the highly connected MWCNT fillers as evidenced by SEM images at fractured surface in Figs. S1 and S2. The well-formulated MWCNT networks, which have positive effect on the electrical conductivity of nanocomposites, can affect an adverse influence on the piezoresistive sensitivity, in which the related results are observed in the experimental results in this study.

Fig. 1(c) shows the results of numerical simulations under the uniaxial tension with different stiffness of nanocomposites. It is found in the figure that the electrical resistance change tends to decrease as the effective stiffness of nanocomposites increases. Clearly, it is likely that the deformation resistance of the nanocomposite systems is gradually enhanced when $\mathbf{C}^*$ increases, ultimately decreasing the change of electrical resistance. The predicted electrical conductivities with various values of interfacial resistivity (ρ_0) are also rendered in Fig. 1(d). A piezoresistivity response is noted when the interfacial resistivity increases in the present model, whereas a weak electrical resistance change of the nanocomposite is predicted at a state with lower interfacial resistivity. Similarly, the weaken stiffness of nanocomposite and the low level of interfacial resistivity at the region between MWCNTs/matrix result in an increase in the piezoresistive sensitivity as observed in the literature [20,27,34,45]. These results are in good agreement with the above-mentioned studies, demonstrating that the potential capability of predictions of the introduced model.

To investigate the effects of the model constants on the effective electrical conductivity further, nanocomposites with varying interface resistivity levels (ρ_c) and average tensile strain ($\bar{\varepsilon}$) values were numerically simulated. As shown in Fig. 2(a), the effective electrical conductivity of the nanocomposites is reduced when the value of ρ_c increases. The cause of such simulation results is quite clear: the definition of ρ_c considered in this study is that pertaining to thinly coated interface resistivity on the MWCNT surface, which acts to reduce the conductivity of the MWCNT filler. Hence, the original electrical conductivity of MWCNTs are simulated as the ρ_c value becomes smaller. By the same principle, as a higher ρ_c value is applied, lower electrical conductivity of the MWCNTs is calculated, and this ultimately lowers the predicted effective electrical conductivity of the nanocomposites.

In addition, Fig. 2(b) shows the theoretical results from the

present formulation in which the nanocomposite is constantly being extended by a certain value of $\bar{\varepsilon}$. In practice, it would take a great deal of experimentation to obtain these values; however, they can be easily predicted through the present proposed model. When tensile stresses are applied to the nanocomposite, the electrical network in the matrix becomes disconnected and the effective electrical conductivity value is reduced as well. The deformation also causes micro/nano-cracks in the nanocomposite, and these cracks also lead to lower values of the electrical conductivity.

3. Experimental validation

3.1. Materials and sample preparation

In this research work, commercial MWCNTs were purchased from Wonil Corporation, South Korea, in the average sizes of 4–5 nm and 100 μm in diameter and length, respectively. N-methy1–2-pyrrolidone (NMP), as a proprietary product of Sigma-Aldrich, was used in order to fabricate the nanocomposite films. The poly-amic acid (PAA) was obtained as a result of the in-situ polymerization of 3,3'-dihydroxybenzidine (DHB) and pyromellitic dianhydride (PDMA), as monomers. DHB and PMDA were purchased from TCI, Japan, and Lonza, China, accordingly. All of the above mentioned materials were used as received without any further purification.

The various types of nanocomposite films were fabricated using the following process: As shown in Fig. 3, MWCNTs were dispersed in NMP with the aid of bath-type and horn-type sonicators for 1 h at room temperature. Afterwards, the solution was mixed with DHB and stirred for 1 h. Subsequently, PMDA was added to the mixture and the resultant solution was stirred for 24 h. As shown in Fig. 3, the nanocomposite solutions were dropped on the surface of a substrate (PI film) and then, the Doctor-blading method was used in order to make thin nanocomposite films on a substrate. In this method, the final PAA solution of nanocomposites was casted on commercial polyimide films and form thin films with the aid of a moving bar at the specified speed and thickness. Here, the nanocomposite films were formed with the bar speed of 0.36 mm/min and initial thickness of 1 mm. This thickness of the films was dramatically decreased during drying process in a vacuum oven at 90 °C for 2 h. In order to fabricate the MWCNT/PI films, the dried PAA films were detached from the PI substrates and placed in a furnace with a gradual heating program in an Ar environment. The heating program can be found in Ref. [31]. This process was repeated for all of the nanocomposite films. The ratios for the fabrication of nanocomposites are listed in Table 1.

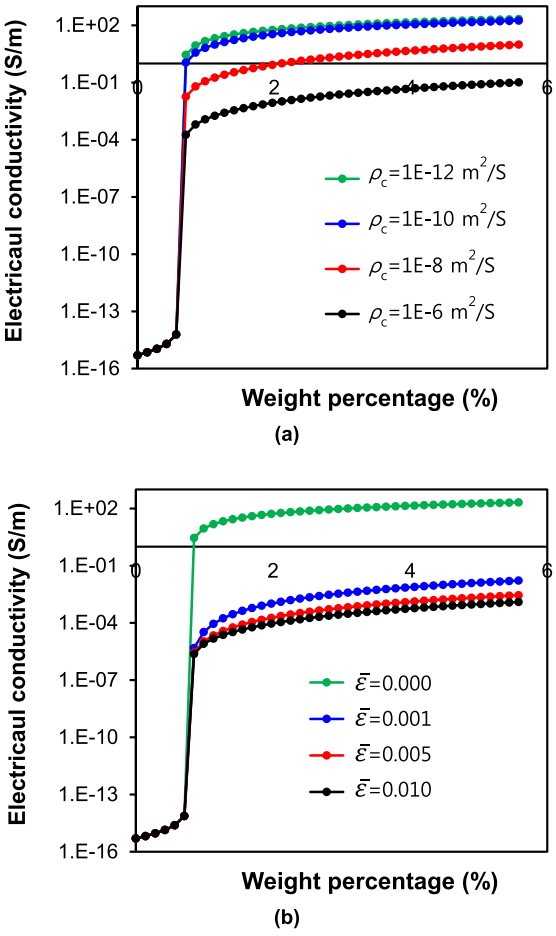

Fig. 2. The effective electrical conductivity of polymer nanocomposites versus content of MWCNT filler for different (a) interface resistivity (ρc) and (b) averaged strain ($\bar{\varepsilon}$) values. (A colour version of this figure can be viewed online.)

3.2. Test methods

In order to measure the DC sheet resistance of the nanocomposite films, a four-point probe method (FPP-RS8, DasolEng, Korea) was employed; as shown in Fig. S3, four-point probe based instruments can be used to measure the average sheet resistance of a thin film by passing current through the outside two points of the probe and measuring the voltage across the inside two points. Since the distance between the probes of the sheet resistance measurement device is equal, the DC electrical conductivity of the thin films was calculated in accordance with the following equations in below:

$$R_{sheet} = \frac{\frac{\pi}{ln(2)} V}{I} = 4.53\left(\frac{V}{I}\right), \quad \rho = R_{sheet} \cdot t, \quad \sigma = \frac{1}{\rho} = 1/(R_{sheet} \cdot t) \tag{9}$$

where σ (S/m) denotes the electrical conductivity; V and I are the voltage and current read by the sheet resistance measurement device, respectively; ρ (Ω.m) is the bulk resistivity; t (m) indicates the film thickness; R_{sheet} (Ω) is the DC sheet resistance of the films. It is important to note that the sheet resistance values (R_{sheet}) were directly read by the device shown in Fig. S3. The mechanical properties of MWCNT/PI nanocomposites were characterized by a universal testing machine (UTM, 5567A, Instron). For this purpose, the films were fabricated with the sizes of 25 mm of length and 5 mm of width. The average thickness of the nanocomposite films with 0.5, 1, 2, 3, and 5 wt% of MWCNTs was 60, 55, 63.5, 74.5, and 100 μm, respectively. The samples underwent tensile load up to breaking point with the extension rate of 5 mm/min. The DC electrical resistance change of the nanocomposite specimens under tensile strain was monitored using a two-point probe method that involves connecting two wires to respective electrodes attached to the surface of each end of the nanocomposite films and monitored by a digital multi-meter (DMM) (CH Instruments, Electrochemical Workstation, CHI901D). The experimental setup for the sheet resistance measurement of the films was different compared to that of measuring electrical resistance change. Thus, due to the complexity of the setup for the electrical resistance change measurement, the two-point probe method was employed, as shown in Fig. 4. In order to minimize the contact resistance between the electrodes and the nanocomposite films during the piezoresistive sensing tests, silver paste was coated on the contact area and dried

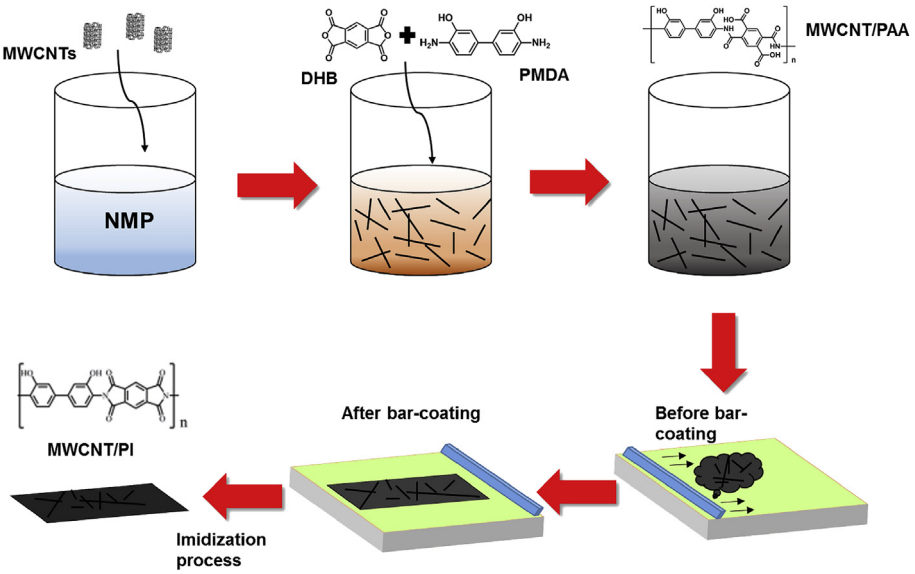

Fig. 3. Schematic view of fabrication process of MWCNTs/PI nanocomposites. (A colour version of this figure can be viewed online.)

Table 1
The constituent materials and their ratios for fabrication of the nanocomposites.

Nanocomposite	DHB (gr)	PMDA (gr)	MWCNT (gr)	NMP (gr)
Pure PI	1.98276	2.00000	0.00000	52.91384
0.5 wt% MWCNT/PI	1.98276	2.00000	0.02001	53.17973
1.0 wt% MWCNT/PI	1.98276	2.00000	0.04023	53.44832
2.0 wt% MWCNT/PI	1.98276	2.00000	0.08128	53.99371
3.0 wt% MWCNT/PI	1.98276	2.00000	0.12317	54.55036
5.0 wt% MWCNT/PI	1.98276	2.00000	0.20962	55.69878

in an oven prior to the tests.

A uniform uniaxial tensile strain for 5 cycles with a maximum value of 4.76% was applied by a horizontal motorized moving stage (Future Science Motion Controller, FS100801A1P1) at a displacement rate of 0.1 mm/s while the electrodes were connected to the DMM. After each half of a cycle, the applied strain was fixed for 10 s. Meanwhile, the data was synchronously stored on a computer. The recorded strain data using the horizontal motorized moving stage is considered as the averaged strain which applies to specimens. Fig. 4 illustrates the experimental setup for measuring the piezoresistivity of the MWCNT/PI nanocomposites. Note that copper tape was attached to the surfaces of both ends of the film and electrodes using silver paste as a compound for the improvement of the contact between electrodes and the surface of the films. The fabricated nanocomposite sensor used in this study is shown in Fig. 5. The morphology of the fractured cross-section of the nanocomposites was studied through scanning electron microscopy (Nova NanoSEM, FEI, USA).

3.3. Experimental results

The electrical characteristics of the various nanocomposites with regard to different MWCNT weight percentages were evaluated through the obtained sheet resistance data. The four-point probe method was chosen to measure the sheet resistance of the nanocomposite films. Thus, the electrical conductivity values of the various types of films were calculated in accordance with Eq. (9). The obtained results are shown in Fig. 6. The electrical conductivity of the pure PI was not measurable; however, the value was reported as 1.17E-15 S/m by Ref. [46].

As shown in Fig. 6, the electrical conductivity of the nanocomposites increased as the filler weight percentages increased. We noticed that the electrical conductivity values had a significant increase in a range of 0.5–1 wt% of MWCNTs. Moreover, Fig. 6 clearly represents the percolation behavior of the nanocomposites where MWCNTs are linked within the matrix material. The percolation threshold of the MWCNT/PI nanocomposites can be estimated using the percolation theory in accordance with Eq. (10) as follows:

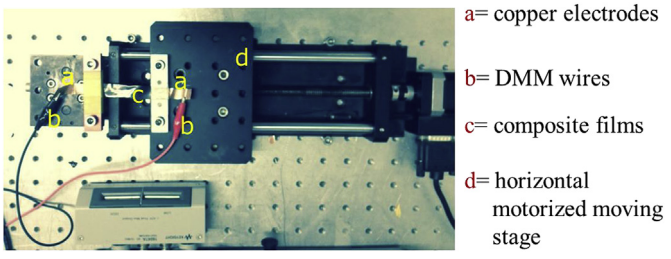

Fig. 4. The experimental setup for evaluation of the piezoresistive properties. (A colour version of this figure can be viewed online.)

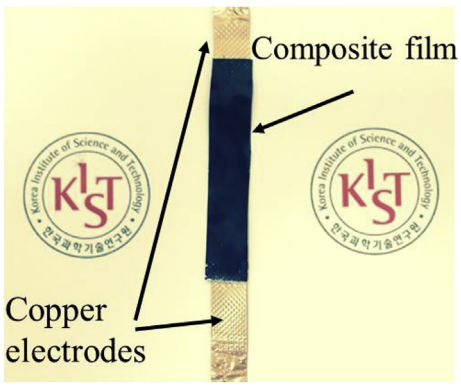

Fig. 5. The actual view of the piezoresistive sensor made of 3 wt% of MWCNTs in PI matrix. (A colour version of this figure can be viewed online.)

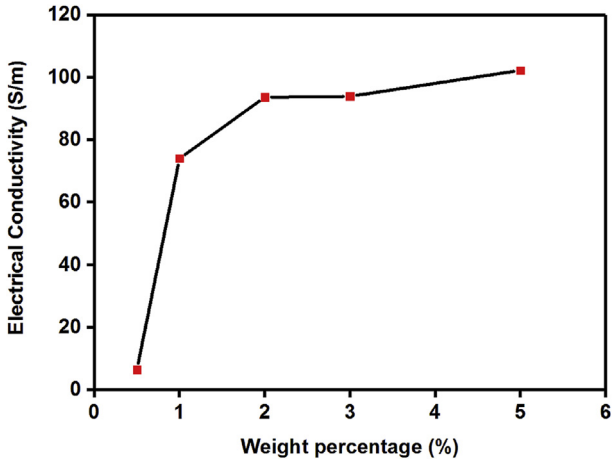

Fig. 6. The electrical conductivity of nanocomposites versus MWCNTs weight percentage. (A colour version of this figure can be viewed online.)

$$\sigma^* = \sigma_f(\varphi - \varphi_c)^t \tag{10}$$

where σ^* and σ_f denote the electrical conductivity of the nanocomposites and the filler, respectively. φ and φ_c represent the filler volume fraction and percolation threshold of the nanocomposites, accordingly. At last, t is the critical exponent. Note that Eq. (10) is valid only when $\varphi - \varphi_c > 0$ is satisfied. Based on the fitted curve using Eq. (10) on the obtained data, the percolation threshold of the nanocomposites was found to be 0.48 wt%, where the parameters σ_f, and t were set to be 573 S/m and 0.44, respectively. Furthermore, the highest value of electrical conductivity was found to be 102 S/m correlated to 5 wt% of MWCNTs.

After the addition of 2 wt% of MWCNTs, the electrical conductivity values almost leveled off by adding more filler. These results were comparable to those from the aforementioned literature [31,46,47]. These results support the idea that the in situ polymerization process could enhance the interfacial interaction between the filler and PI matrix, which effectively improves the electrical conductivity of the nanocomposites [48]. Several reports in the literature confirmed the fact that the use of in-situ polymerization could effectively lower the percolation threshold of the nanocomposites and improve the electrical conductivity of the nanocomposites by providing homogeneous dispersion of the filler with matrix material [45,46,49]. In addition, these studies showed that the use of in-situ polymerization could effectively enhance the interaction between filler and matrix materials that could increase the mechanical properties of the nanocomposites [50].

In order to understand the interfacial interaction between the filler and matrix, Fig. 7 presents the cross-sectional scanning electron microscope (SEM) image of the fractured pure PI as well as 1 and 3 wt% of MWCNTs embedded in PI nanocomposite films. As it can be seen in Fig. 7(a), the fractured surface of the pure PI film was mostly smooth. In contrast, the fractured surface of the 1 and 3 wt% of MWCNT/PI nanocomposite films was rough, which might be due to the strong interfacial interaction of the filler and matrix, as suggested by Ref. [31]. In the case of 1 wt% of MWCNT/PI nanocomposite films, the matrix material could wet the surface of MWCNTs within the matrix, as shown in Fig. 7(b). On the other hand, the high amount of MWCNTs (3 wt%) was not completely wet by the PI due to the exceedingly large surface area of MWCNTs. This could result in the formation of the MWCNTs bundles in some parts of the nanocomposite films (Fig. 7(c)). Overall, both the 1 and 3 wt% of MWCNT/PI nanocomposite films represented the homogenous dispersion of filler among the PI matrix, which was due to the proper fabrication method. The SEM images corresponded to the 1 and 3 wt% of MWCNT/PI nanocomposites with the higher magnification can be found in the supporting information (Figs. S1, S2).

Fig. 8 exhibits the applied stress versus extension of the nanocomposite films. It notes that the five specimens were fabricated by following the ASTM standard [51], and the averaged values were illustrated in the figure. As shown, the tensile strength of the nanocomposites increased compared to the pure PI as the filler weight percentages increased up to 1 wt%. However, the strength of the nanocomposites started decreasing with the further addition of MWCNTs. The tensile strength of the 1 wt% of MWCNTs within PI showed the highest tensile strength among all nanocomposite films, and this value was improved by 100.70% from 145.15 to 291.37 MPa compared to that found for pure PI. This dramatic improvement could be due to the well dispersion of MWCNTs within PI and the strong bond between the fillers and matrix. Nevertheless, using higher ratios of MWCNTs were not shown to be very effective on the mechanical properties of the nanocomposites.

The tensile strength of the nanocomposites decreased for the cases of 2, 3, and 5 wt% of MWCNTs incorporated in PI compared to that of 1 wt% of MWCNT/PI nanocomposite films; however, all of the nanocomposite films showed higher tensile strength compared to the pure PI films. This phenomenon can be due to the lack of interfacial interaction between the fillers and PI matrix in the case of an existence of higher amounts of MWCNTs. In other words, the great surface area of MWCNTs results in the formation of more MWCNTs bundles and aggregation since the fillers would not be well wet by the matrix, which could lead to lowering the interfacial interaction between the polymer and the filler and phase separation. Thus, the degradation of the mechanical properties for the nanocomposite with higher amounts of fillers occurs.

In this study, the piezoresistivity of the 1 and 3 wt% of the MWCNTs embedded PI nanocomposite films with the size of 12 mm in width and 70 mm in length were investigated. These samples were chosen with the consideration of filler ratios close and far to the percolation threshold of the nanocomposites so that their DC electrical resistance change could be detected using the experimental setup shown in Fig. 4. The change in resistance versus applied tensile strain for the samples is depicted in Fig. 9. As shown, the electrical resistance of both samples was linearly increased when the tensile strain was applied and followed the cycles of the tensile strain curve in phase without a considerable time lag or hysteresis.

Fig. 9(a) shows that the maximum change in the electrical resistance of 1 wt% MWCNT/PI nanocomposite films was 0.87% at a maximum applied tensile strain of 4.76%. This nanocomposite had the filler ratio close to the percolation threshold. On the other hand, the maximum electrical resistance change value of 3 wt% of MWCNTs within PI nanocomposite films was obtained at 0.39%, under the same applied tensile strain condition, as shown in Fig. 9(b). Moreover, the results for the 3 wt% of MWCNTs embedded PI nanocomposite films had greater noise compared to that of the 1 wt% of MWCNT/PI nanocomposite films. Hence, it can be concluded that the nanocomposite films with filler ratio close to the percolation threshold led to a higher electrical resistance change compared to those that were far from the percolation threshold. These findings were also reported in several research works available the literature [22,25,29]. In summary, this behavior can be corresponded to the tunneling effect near the percolation threshold of the nanocomposites.

The tunneling effect can be greatly observed in nanocomposites owing conductive filler weight percentages close to the percolation threshold of the nanocomposites; nevertheless, this effect vanishes with the further addition of conductive fillers. In detail, the distance

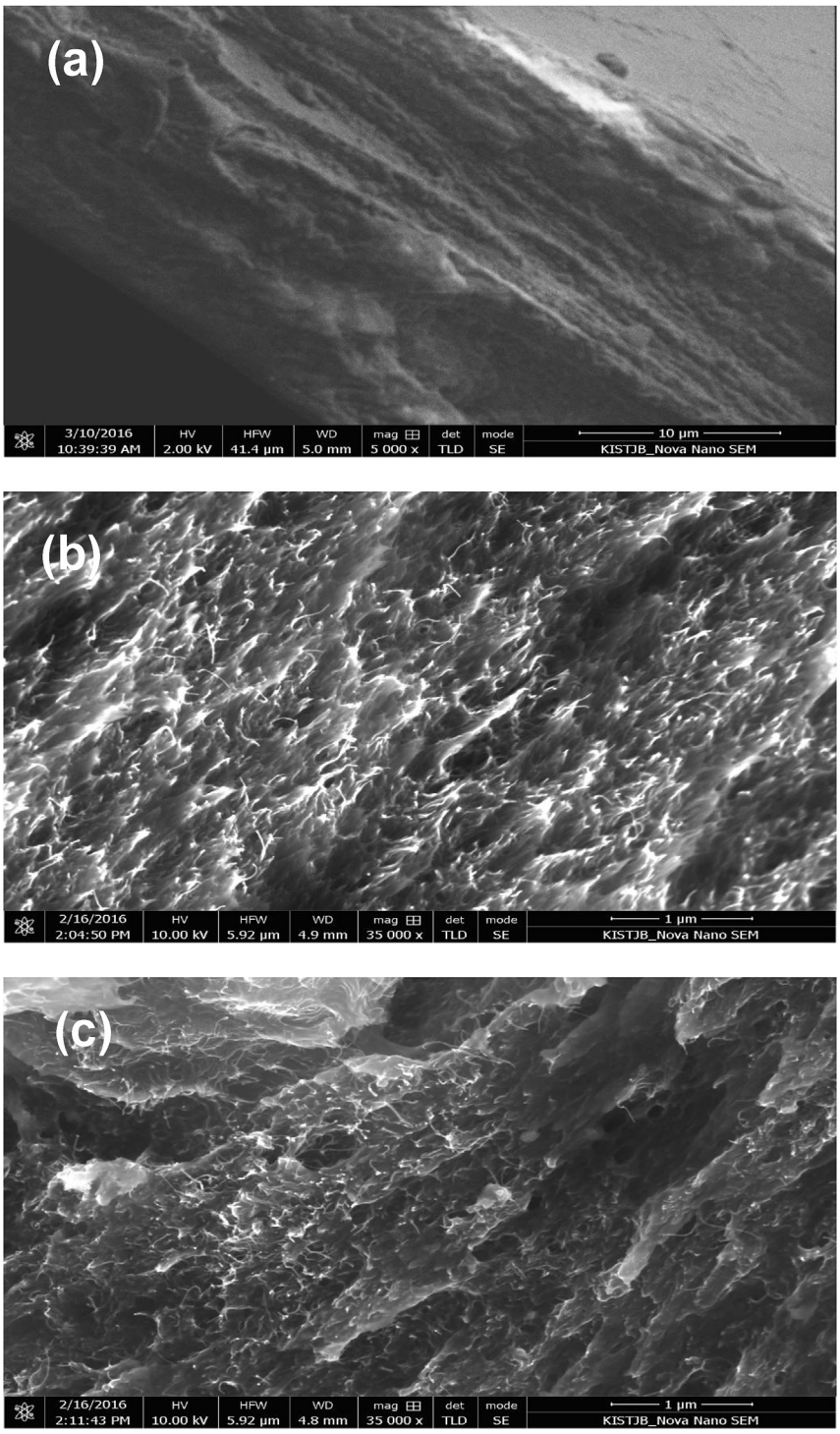

Fig. 7. SEM images taken from the fractured surface of (a) pure PI, (b) 1 wt% of MWCNTs/PI, and (c) 3 wt% of MWCNTs/PI nanocomposites.

between neighboring MWCNTs gradually increases under the applied tensile strain, resulting in the increase of tunneling resistance. Given that, the total electrical resistance of the nanocomposites will also increase. Another reason for the increase in electrical resistance of the nanocomposites is the breakdown of the conducting network of MWCNTs under lower levels of applied strain. On the other hand, for the nanocomposites with filler concentration far from the percolation threshold, the conductive networks are already linked and, thus, the applied tensile strain would not significantly change the electrical resistance of the nanocomposite. As a result, the incorporation of 1 wt% of MWCNTs, which is right after the percolation threshold, within the PI matrix could present greater amounts of electrical resistance change than that of the 3 wt% MWCNT/PI nanocomposite films [25,29].

Another factor to examine the strain sensors could be the piezoresistive strain coefficient or gauge factor (GF). This value can be calculated via $GF = \Delta R / R0 \cdot \varepsilon$, where ΔR represents the electrical resistance change, R_0 denotes the initial resistance before applying

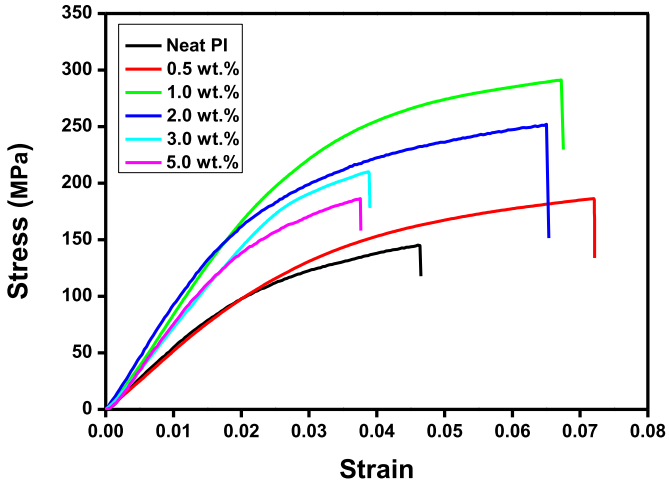

Fig. 8. Stress versus displacement curves for nanocomposite films containing various weight percentages of MWCNTs. (A colour version of this figure can be viewed online.)

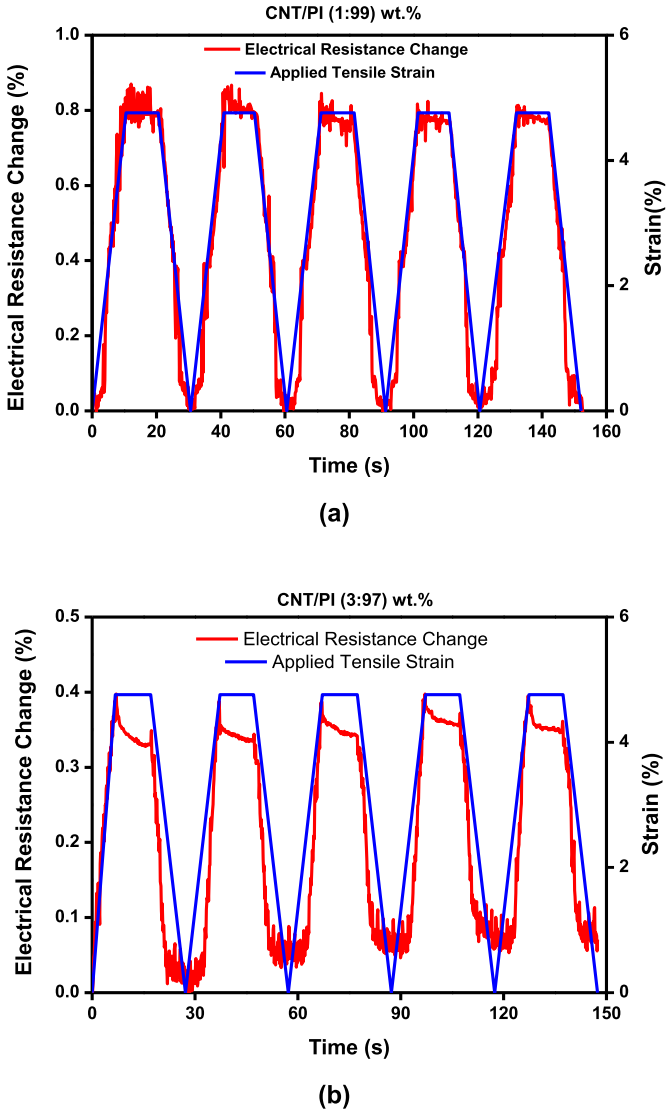

Fig. 9. The electrical resistance change of (a) 1 wt% (a) and (b) 3 wt% of MWCNTs within PI nanocomposites versus applied tensile strain. (A colour version of this figure can be viewed online.)

external load/strain, and ε is strain. The GF for 1 and 3 wt% of MWCNTs incorporated in PI matrix was calculated to be 0.18 and 0.08, respectively. These values were comparatively lower than the ones reported in the literature as summarized in Ref. [35]. Overall, the CNT based piezoresistive nanocomposites shows lower GF values compared to the other conductive filler such as Ag-nanowires (NWs), graphene, and carbon black. Here, the use of PI as a non-soft matrix might be another reason for the low values of GFs.

4. Experimental comparisons

The experimental comparisons between the present experiment data on MWCNTs embedded polyimide nanocomposites and predictions are made to highlight the predictive capability of the effective medium theory-based model. The same material properties of the MWCNTs and PI matrix as those in the experiment and the numerical simulation section as: $\sigma_0 = 5E\text{-}15$ S/m, $\sigma_1 = 1.943E4$ S/m, $L = 100$ μm, $D = 4.5$ nm. It is noted that the same interface parameter ($\rho_0 = 1E\text{-}4$ m^2/S) and the stiffness constants previously measured are applied to all the cases of comparisons to verify the model.

The predicted piezoresistive responses of the nanocomposites based on the above material properties and parameters are displayed in Fig. 10(a) and (b). Here, the volume fractions of MWCNTs are respectively 1 and 3%, and the density of the matrix and MWCNTs are considered as 1.48 and 2.10 g/cc for weight-volume fraction conversion. The material densities are experimentally measured in the present study, and the values are confirmed to be similar to those reported by the previous literature [52–55]. The good correlations between experiment data and the present prediction are observed, whereas a slight deviation is predicted from the simulations after 3–5 cycles.

The reason for these results is believed to be that the damage and/or plasticity behaviors in nanocomposites occur during the repetitive uniaxial tensile test. The present model is developed within the consideration of the elastic region; however, the accuracy of the analysis is expected improve when the additional mechanisms (*e.g.*, micro/nano-crack, debonding damage, matrix plasticity, *etc.*) are incorporated into the present framework. To extend the present model to cover the above-mentioned phenomena, additional theoretical approaches such as the Weibull's probability damage model [56], the continuum model for crack nucleation [57], and the yield criterion with isotropic hardening law [58] would be taken into account in the future work.

To further demonstrate the applicability of the proposed model, the prediction of electrical conductivity with varying MWCNTs weight percentages is compared with experimentally measured data, as shown in Fig. 11. Overall, the predicted simulation results and the experimental data match well. In addition, it should be noted that the same material and model parameters previously used are utilized in this comparison for the demonstration purpose.

From the aforementioned numerical simulations and experimental comparisons, it can be concluded that the piezoresistive response and electrical conductivity with various conditions are described well based on the present model. Although the interface constant cannot be explicitly calculated in the present study, the same estimated ρ_0 value for the constant is applied to the various conditions in Figs. 10(a) and (b), and 11, showing good agreements between experimental observations and predictions. These results imply that the proposed method is expected to offer a various range of predictive capacity of electrical properties for nanocomposites. It can also be presumed from the present study that the excessive electrical conductivity of nanocomposites is, of course, advantageous in terms of electrical stability; however, it may decrease the sensitivity of the piezoresistive response that can operate as a strain

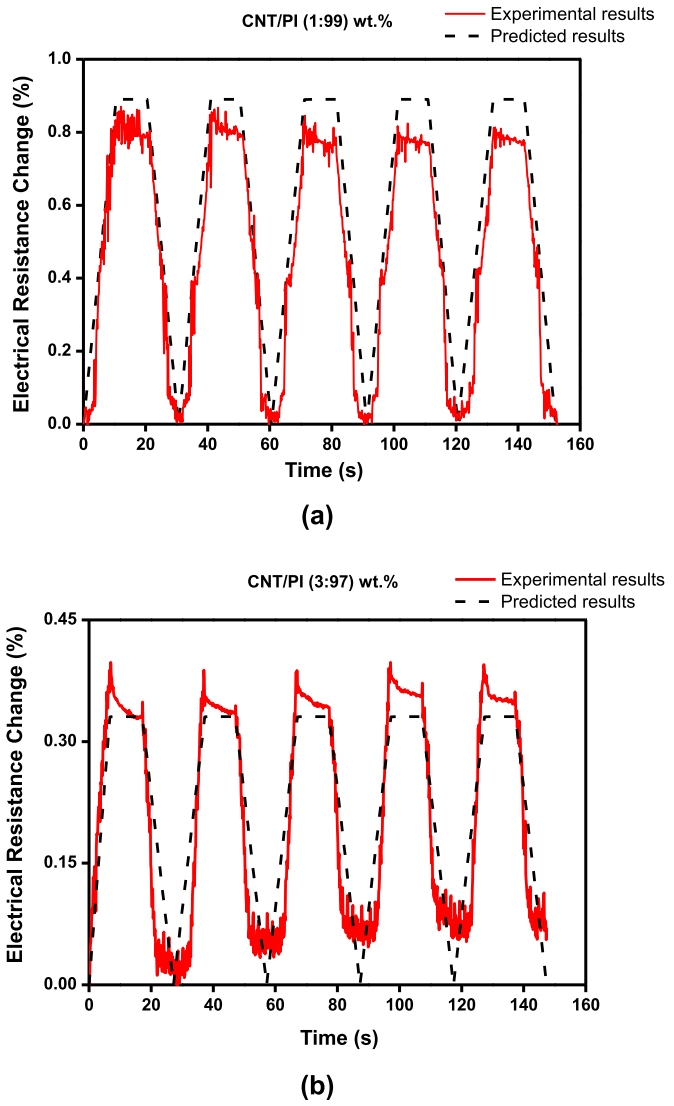

Fig. 10. The comparisons of electrical resistance change curves between the present prediction and the experimental data of (a) MWCNT/PI (1:99) and (b) MWCNT/PI (3:97). (A colour version of this figure can be viewed online.)

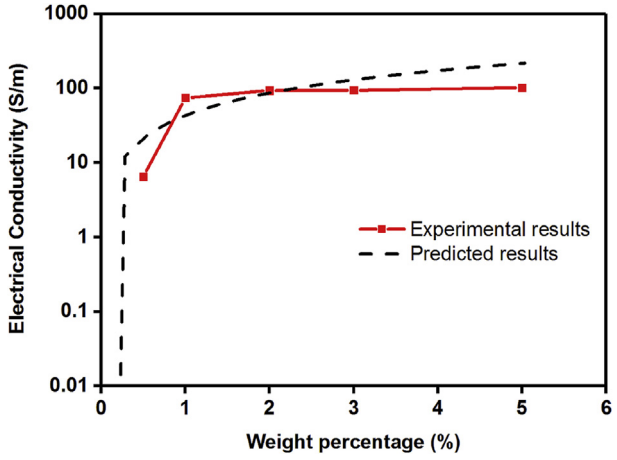

Fig. 11. Comparison of the electrical conductivity with the experimental data and the present prediction for MWCNTs-reinforced polyimide nanocomposite films. (A colour version of this figure can be viewed online.)

sensor. The balance among each parameter would be, therefore, critical for the optimal design of nanocomposites.

5. Conclusions

In conclusion, we have completed theoretical and experimental studies to elucidate the piezoresistive response of MWCNT/polymer nanocomposite films. Based on the self-consistent scheme, a series of numerical simulations and experimental comparisons was also performed. The successful analysis of the piezoresistive responses by the theoretical model and experimental tests yields that enables us to predict the effective electro-mechanical behaviors of MWCNTs-reinforced polymeric nanocomposites, which can be portrayed based on the analytical approximation for nanocomposite modeling. The important features and findings from the present study can be summarized as follows:

- The piezoresistive response and electrical conductivity with various conditions (*e.g.*, the level of applied tensile strain, MWCNT weight percentage, and length of MWCNTs) are described based on the developed framework.
- The tensile strength of the nanocomposites increased compared to the pure PI as the filler weight percentages increased up to 1 wt%; however, the strength of the nanocomposites started decreasing with the further addition of MWCNTs.
- It is observed from the test results that the nanocomposite films with MWCNTs slightly above the percolation threshold (below 1 wt%) shows the most sensitivity to external deformation than those of far above the percolation point.
- Three sets of comparisons between experimental data and present predictions were performed, and their good correlations demonstrated the predictive capability of the present model.

The obtained findings signify that the piezoresistive response is not proportional to the improvement of electrical and mechanical properties, and the proposed model can play a role in predicting the physical changes by CNT fillers under various cases and conditions.

Acknowledgement

This study was supported by the Korea Institute of Science and Technology (KIST) Institutional Program & Open Research Program and by Nano·Material Technology Development Program through the National Research Foundation of Korea (NRF) funded by the Ministry of Science, ICT and Future Planning (2016M3A7B4027695).

Appendix A. Supplementary data

Supplementary data related to this article can be found at http://dx.doi.org/10.1016/j.carbon.2017.05.059.

References

[1] Q. Jiang, X. Wang, Y. Zhu, D. Hui, Y. Qiu, Mechanical, electrical and thermal properties of aligned carbon nanotube/polyimide composites, Compos. Part B Eng. 56 (2014) 408–412.
[2] J. Tiusanen, D. Vlasveld, J. Vuorinen, Review on the effects of injection moulding parameters on the electrical resistivity of carbon nanotube filled polymer parts, Compos. Sci. Technol. 72 (14) (2012) 1741–1752.
[3] S.Y. Kim, Y.J. Noh, J. Yu, Prediction and experimental validation of electrical percolation by applying a modified micromechanics model considering multiple heterogeneous inclusions, Compos. Sci. Technol. 106 (2015) 156–162.
[4] B. Yang, Jang J-u, S.-H. Eem, S.Y. Kim, A probabilistic micromechanical modeling for electrical properties of nanocomposites with multi-walled carbon nanotube morphology, Compos. Part A Appl. Sci. Manuf. 92 (2017) 108–117.
[5] J. Lee, S. Kim, J. Lee, D. Yang, B.C. Park, S. Ryu, et al., A stretchable strain sensor

based on a metal nanoparticle thin film for human motion detection, Nanoscale 6 (20) (2014) 11932–11939.
[6] C. Li, E.T. Thostenson, T.-W. Chou, Sensors and actuators based on carbon nanotubes and their composites: a review, Compos. Sci. Technol. 68 (6) (2008) 1227–1249.
[7] B. Yang, H. Shin, H. Lee, H. Kim, A combined molecular dynamics/micromechanics/finite element approach for multiscale constitutive modeling of nanocomposites with interface effects, Appl. Phys. Lett. 103 (24) (2013) 241903.
[8] G. Kim, B. Yang, G. Ryu, H. Lee, The electrically conductive carbon nanotube (CNT)/cement composites for accelerated curing and thermal cracking reduction, Compos. Struct. 158 (2016) 20–29.
[9] Y. Wang, G.J. Weng, S.A. Meguid, A.M. Hamouda, A continuum model with a percolation threshold and tunneling-assisted interfacial conductivity for carbon nanotube-based nanocomposites, J. Appl. Phys. 115 (19) (2014) 193706.
[10] R. Hashemi, G.J. Weng, A theoretical treatment of graphene nanocomposites with percolation threshold, tunneling-assisted conductivity and microcapacitor effect in AC and DC electrical settings, Carbon 96 (2016) 474–490.
[11] N. Hu, Y. Karube, M. Arai, T. Watanabe, C. Yan, Y. Li, et al., Investigation on sensitivity of a polymer/carbon nanotube composite strain sensor, Carbon 48 (3) (2010) 680–687.
[12] M. Amjadi, A. Pichitpajongkit, S. Lee, S. Ryu, I. Park, Highly stretchable and sensitive strain sensor based on silver nanowire–elastomer nanocomposite, ACS Nano 8 (5) (2014) 5154–5163.
[13] M. Taya, W. Kim, K. Ono, Piezoresistivity of a short fiber/elastomer matrix composite, Mech. Mater. 28 (1) (1998) 53–59.
[14] T. Theodosiou, D. Saravanos, Numerical investigation of mechanisms affecting the piezoresistive properties of CNT-doped polymers using multi-scale models, Compos. Sci. Technol. 70 (9) (2010) 1312–1320.
[15] Q.T. Trinh, G. Gerlach, J. Sorber, K.-F. Arndt, Hydrogel-based piezoresistive pH sensors: design, simulation and output characteristics, Sens. Actuators B Chem. 117 (1) (2006) 17–26.
[16] X. Ren, G.D. Seidel, Computational micromechanics modeling of inherent piezoresistivity in carbon nanotube–polymer nanocomposites, J. Intell. Mater. Syst. Struct. 24 (12) (2013) 1459–1483.
[17] P. Pramanik, D. Khastgir, S. De, T. Saha, Pressure-sensitive electrically conductive nitrile rubber composites filled with particulate carbon black and short carbon fibre, J. Mater. Sci. 25 (9) (1990) 3848–3853.
[18] J. Kost, A. Foux, M. Narkis, Quantitative model relating electrical resistance, strain, and time for carbon black loaded silicone rubber, Polym. Eng. Sci. 34 (21) (1994) 1628–1634.
[19] S. Qu, S.-C. Wong, Piezoresistive behavior of polymer reinforced by expanded graphite, Compos. Sci. Technol. 67 (2) (2007) 231–237.
[20] J. Hwang, J. Jang, K. Hong, K.N. Kim, J.H. Han, K. Shin, et al., Poly (3-hexylthiophene) wrapped carbon nanotube/poly (dimethylsiloxane) composites for use in finger-sensing piezoresistive pressure sensors, Carbon 49 (1) (2011) 106–110.
[21] A. Oliva-Avilés, F. Avilés, V. Sosa, Electrical and piezoresistive properties of multi-walled carbon nanotube/polymer composite films aligned by an electric field, Carbon 49 (9) (2011) 2989–2997.
[22] H. Souri, I. Nam, H. Lee, Electrical properties and piezoresistive evaluation of polyurethane-based composites with carbon nano-materials, Compos. Sci. Technol. 121 (2015) 41–48.
[23] K. Singh, J. Akhtar, S. Varghese, Multiwalled carbon nanotube-polyimide nanocomposite for MEMS piezoresistive pressure sensor applications, Microsyst. Technol. 20 (12) (2014) 2255–2259.
[24] K. Aly, A. Li, P.D. Bradford, Strain sensing in composites using aligned carbon nanotube sheets embedded in the interlaminar region, Compos. Part A Appl. Sci. Manuf. 90 (2016) 536–548.
[25] N. Hu, Y. Karube, C. Yan, Z. Masuda, H. Fukunaga, Tunneling effect in a polymer/carbon nanotube nanocomposite strain sensor, Acta Mater. 56 (13) (2008) 2929–2936.
[26] H. Souri, I. Nam, H. Lee, A zinc oxide/polyurethane-based generator composite as a self-powered sensor for traffic flow monitoring, Compos. Struct. 134 (2015) 579–586.
[27] J. Bautista-Quijano, F. Avilés, J. Cauich-Rodriguez, R. Schönfelder, A. Bachmatiuk, T. Gemming, et al., Tensile piezoresistivity and disruption of percolation in singlewall and multiwall carbon nanotube/polyurethane composites, Synth. Met. 185 (2013) 96–102.
[28] H. Liu, W. Huang, J. Gao, K. Dai, G. Zheng, C. Liu, et al., Piezoresistive behavior of porous carbon nanotube-thermoplastic polyurethane conductive nanocomposites with ultrahigh compressibility, Appl. Phys. Lett. 108 (1) (2016) 011904.
[29] J.H. Kang, C. Park, J.A. Scholl, A.H. Brazin, N.M. Holloway, J.W. High, et al., Piezoresistive characteristics of single wall carbon nanotube/polyimide nanocomposites, J. Polym. Sci. Part B Polym. Phys. 47 (10) (2009) 994–1003.
[30] M.H. Wichmann, S.T. Buschhorn, J. Gehrmann, K. Schulte, Piezoresistive response of epoxy composites with carbon nanoparticles under tensile load, Phys. Rev. B 80 (24) (2009) 245437.
[31] J. Lim, D.G. Shin, H. Yeo, M. Goh, B.C. Ku, C.M. Yang, et al., The mechanical and electrical properties of carbon nanotube-grafted polyimide nanocomposites, J. Polym. Sci. Part B Polym. Phys. 52 (14) (2014) 960–966.
[32] T. Matsuura, Y. Hasuda, S. Nishi, N. Yamada, Polyimide derived from 2, 2'-bis (trifluoromethyl)-4, 4'-diaminobiphenyl. 1. Synthesis and characterization of polyimides prepared with 2, 2'-bis (3, 4-dicarboxyphenyl) hexafluoropropane dianhydride or pyromellitic dianhydride, Macromolecules 24 (18) (1991) 5001–5005.
[33] X. Jia, Q. Zhang, M.-Q. Zhao, G.-H. Xu, J.-Q. Huang, W. Qian, et al., Dramatic enhancements in toughness of polyimide nanocomposite via long-CNT-induced long-range creep, J. Mater. Chem. 22 (14) (2012) 7050–7056.
[34] T. Akhter, S.C. Mun, S. Saeed, O.O. Park, H.M. Siddiqi, Enhancing the dielectric properties of highly compatible new polyimide/γ-ray irradiated MWCNT nanocomposites, RSC Adv. 5 (87) (2015) 71183–71189.
[35] M. Amjadi, K.U. Kyung, I. Park, M. Sitti, Stretchable, skin-mountable, and wearable strain sensors and their potential applications: a review, Adv. Funct. Mater. 26 (2016) 1678–1698.
[36] S. Pyo, H. Lee, Micromechanical analysis of aligned and randomly oriented whisker-/short fiber-reinforced composites, Comput. Model. Eng. Sci. (CMES) 40 (3) (2009) 271.
[37] B. Yang, H. Souri, S. Kim, S. Ryu, H. Lee, An analytical model to predict curvature effects of the carbon nanotube on the overall behavior of nanocomposites, J. Appl. Phys. 116 (3) (2014) 033511.
[38] L.D. Landau, J. Bell, M. Kearsley, L. Pitaevskii, E. Lifshitz, J. Sykes, Electrodynamics of Continuous Media vol. 8, Pergamon Press, Oxford, 1984, pp. 153–157.
[39] D.-L. Shi, X.-Q. Feng, Y.Y. Huang, K.-C. Hwang, H. Gao, The effect of nanotube waviness and agglomeration on the elastic property of carbon nanotube-reinforced composites, J. Eng. Mater. Technol. 126 (3) (2004) 250–257.
[40] K. Yanase, S. Moriyama, J. Ju, Effects of CNT waviness on the effective elastic responses of CNT-reinforced polymer composites, Acta Mech. 224 (7) (2013) 1351–1364.
[41] B. Yang, K. Cho, G. Kim, H. Lee, Effect of CNT agglomeration on the electrical conductivity and percolation threshold of nanocomposites: a micromechanics-based approach, CMES Comput. Model. Eng. Sci. 103 (5) (2014) 343–365.
[42] C.-W. Nan, R. Birringer, D.R. Clarke, H. Gleiter, Effective thermal conductivity of particulate composites with interfacial thermal resistance, J. Appl. Phys. 81 (10) (1997) 6692–6699.
[43] D.S. McLachlan, C. Chiteme, C. Park, K.E. Wise, S.E. Lowther, P.T. Lillehei, et al., AC and DC percolative conductivity of single wall carbon nanotube polymer composites, J. Polym. Sci. Part B Polym. Phys. 43 (22) (2005) 3273–3287.
[44] S.N. Leung, M.O. Khan, E. Chan, H. Naguib, F. Dawson, V. Adinkrah, et al., Analytical modeling and characterization of heat transfer in thermally conductive polymer composites filled with spherical particulates, Compos. Part B Eng. 45 (1) (2013) 43–49.
[45] J. Sandler, J. Kirk, I. Kinloch, M. Shaffer, A. Windle, Ultra-low electrical percolation threshold in carbon-nanotube-epoxy composites, Polymer 44 (19) (2003) 5893–5899.
[46] X. Jiang, Y. Bin, M. Matsuo, Electrical and mechanical properties of polyimide–carbon nanotubes composites fabricated by in situ polymerization, Polymer 46 (18) (2005) 7418–7424.
[47] R. Srivastava, S. Banerjee, D. Jehnichen, B. Voit, F. Böhme, In situ preparation of polyimide composites based on functionalized carbon nanotubes, Macromol. Mater. Eng. 294 (2) (2009) 96–102.
[48] C.-C. Teng, C.-C.M. Ma, K.-C. Chiou, T.-M. Lee, Synergetic effect of thermal conductive properties of epoxy composites containing functionalized multi-walled carbon nanotubes and aluminum nitride, Compos. Part B Eng. 43 (2) (2012) 265–271.
[49] C. Park, Z. Ounaies, K.A. Watson, R.E. Crooks, J. Smith, S.E. Lowther, et al., Dispersion of single wall carbon nanotubes by in situ polymerization under sonication, Chem. Phys. Lett. 364 (3) (2002) 303–308.
[50] R. Sengupta, M. Bhattacharya, S. Bandyopadhyay, A.K. Bhowmick, A review on the mechanical and electrical properties of graphite and modified graphite reinforced polymer composites, Prog. Polym. Sci. 36 (5) (2011) 638–670.
[51] ASTM C127-12, Standard test method for tensile properties of thin plastic sheeting, ASTM Int. (2012).
[52] J.G. Van Alsten, J.C. Coburn, Structural effects on the transport of water in polyimides, Macromolecules 27 (14) (1994) 3746–3752.
[53] T. Maegawa, O. Miyashita, Y. Irie, H. Imoto, K. Naka, Synthesis and properties of polyimides containing hexaisobutyl-substituted T 8 cages in their main chains, RSC Adv. 6 (38) (2016) 31751–31757.
[54] H. Miyagawa, M.J. Rich, L.T. Drzal, Thermo-physical properties of epoxy nanocomposites reinforced by carbon nanotubes and vapor grown carbon fibers, Thermochim. Acta 442 (1) (2006) 67–73.
[55] Y. Kim, T. Hayashi, M. Endo, Y. Kaburagi, T. Tsukada, J. Shan, et al., Synthesis and structural characterization of thin multi-walled carbon nanotubes with a partially facetted cross section by a floating reactant method, Carbon 43 (11) (2005) 2243–2250.
[56] W. Weibull, A statistical function of wide distribution, J. Appl. Mech. 18 (1951) 293–297.
[57] B. Karihaloo, D. Fu, A damage-based constitutive law for plain concrete in tension, Eur. J. Mech. A Solids 8 (5) (1989) 373–384.
[58] P. Ludwik, R. Scheu, Ueber kerbwirkungen bei flusseisen, Stahl u Eisen 43 (1923) 999–1001.
[59] G.M. Kim, B.J. Yang, K.J. Cho, E.M. Kim, H.K. Lee, Influences of CNT dispersion and pore characteristics on the electrical performance of cementitious composites, Compos. Struct. 164 (2017) 32–42.
[60] H. Jeon, Y. Jaesang, L. Hunsu, G.M. Kim, J.W. Kim, Y.C. Jung, et al., A combined analytical formulation and genetic algorithm to analyze the nonlinear damage responses of continuous fiber toughened composites, Comput. Mech. (2017) 1–16.